Open Chemistry Journal

BENTHAM OPEN

Design and Synthesis of Some Imidazolyl Derivatives: Photophysical Studies and Application in Detection of Anions

Mohammad Shahid, Rashid Ali, Syed S. Razi, Priyanka Srivastava, Ramesh C. Gupta, Sushil K. Dwivedi, Arvind Misra[*]

Open Chemistry Journal, Volume 2, 2015

ISSN: 1874-8422
DOI: 10.2174/1874842220150608E001

Article Type: Research Article

Received: April 03, 2015
Revised: May 10, 2015
Accepted: May 26, 2015

Provisional PDF Publication Date: June 24, 2015

Design and synthesis of some imidazolyl derivatives: Photophysical studies and application in detection of anions

Mohammad Shahid†, Rashid Ali†, Syed S. Razi, Priyanka Srivastava, Ramesh C. Gupta, Sushil K. Dwivedi, Arvind Misra*

Department of Chemistry, Faculty of Science, Banaras Hindu University, Varanasi – 221 005. UP. INDIA.

Corresponding author email: arvindmisra2003@yahoo.com; amisra@bhu.ac.in

Abstract

A fluorescent probe based on dicyanovinylphenanthroimidazole (**DCPPI**) has been designed and synthesized and its potential application to recognize F^- and CN^- ions via different channels has been tested in different medium. **DCPPI** shows intramolecular charge transfer process and exhibit ratiometric response toward F^- and CN^- ions. The change in physicochemical properties of **DCPPI** in the presence of cyanide can be attributed to the formation of Michael type adduct, **DCPPIA** whereas both F^- and CN^- ions have shown affinities to interact with NH fragment of imidazolyl unit under the condition. The possible mode of interaction has been confirmed by absorption, emission, NMR and ESI-MS spectral data analysis.

Graphical Abstract

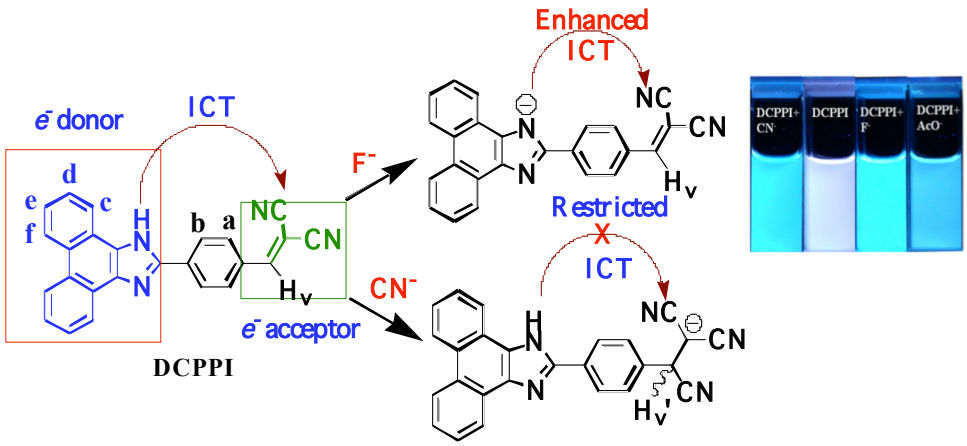

Keywords: DCPPI, F^- ,CN^- and DCPPIA

Notes: †Authors have made equal contribution

1. Introduction

The recognition and sensing of anions have attracted considerable current interest owing to their active involvement in a variety of biological, environmental and industrial processes [1-12]. For instance, fluoride is valuable in the treatment of osteoporosis and dental care however, its high concentration may cause serious health problems such as fluorosis, nephrotoxic changes in organisms and even urolithiasis [13,14]. Cyanide is known detrimental anion that is widely used in various industrial projects such as, gold extraction, electroplating, etc [14]. A small amount of cyanide is lethal to human body due to its strong affinity with the active site of cytochrome a_3 that may inhibit cellular respiration in mammals [7-12]. The sources of cyanide in water are discharge from chemical industries, metal mining processes, and waste water treatment facilities [7-12]. Cyanide has also been used as a chemical warfare agent and even as a terror material [7-12]. Therefore, detection of anions particularly, fluoride and cyanide at low concentration is demanding.

In recent past various research groups have given more emphasis to develop good receptor systems based on synthetic small organic molecules and scaffolds to detect anions accurately [1-18]. For an effective and successful anion recognition event the choice of potential ionophore is crucial because specific geometry, high electronegativity, basicity and nucleophilicity of different class of anions interact with an ionophore differently either by hydrogen bonding interaction, deprotonation and possible nucleophilic addition reactions. Consequently, the typical photophysical behavior encountered due to structural change in a receptor system can be easily followed by spectroscopic techniques like absorption, emission and NMR [19-29].

Some novel receptor system based on boron [30,31] and silicon [32] derivatives, quantum dots [33], mesoporous silica material [7-12], and BODIPY [34] have been successfully utilized to detect anions by hydrogen bonding [35-39], coordination or covalent bonding interactions [40-42]. Similarly, ensemble based demetallization of copper by cyanide has also been utilized to detect cyanide-displacement approach [15-17]. The sensing methods involving H-bonding interaction to detect CN^- have limitations in the environment of competitive anions [15-17]. Similarly, most of sensing approach to recognize fluoride show fluorescence quenching and examples to detect both F^- and CN^- ions through intramolecular charge transfer (ICT) mechanism and ratiometric fluorescence response are highly demanding and are limited in number [1-10]. The advantages of ratiometric measurements enlarges the scope of fluorescent sensors by increasing

the dynamic range and provision for a built-in correction for environmental effects and its application in areas such as medicine, industry and the environment [6]. Therefore, the design and synthesis of a small organic molecular system that is capable to recognize anions selectively with a sensitive naked eye detectable change and unique photophysical behavior is worthy to investigate. In the same interest our research group is trying to develop some efficient and versatile organic molecular scaffold to detect anions, cations, and biomolecules through fluorescence enhancement, "turn-on response" [43-66]. We herein report design and synthesis of some phenanthrene derivatives in which 2,2-dicyanovinylphenanthroimidazole (**DCPPI**) has worked as an efficient, selective and sensitive dual anion responsive intramolecular charge transfer (ICT) probe to recognize F^- and CN^- ions via different channels. **DCPPI** upon interaction with different anions has shown ratiometric response for F^- and CN^- ions in acetonitrile (MeCN) and high selectivity for CN^- in semiaqueous medium (H_2O-MeCN; 50%).

2. Results and Discussion

2.1. Design and synthesis of target molecules

Phenanthroimidazole based systems due to the dramatic supramolecular properties, stability, ease of synthesis, a high extinction coefficient and tuneable photophysical properties have been explored as potential chromophores in a molecular-tweezers system for explosives [45], amine sensors [46,47], fluorophore in a super-radiant laser dye [48], fluorescent tag [49], OLED materials [50-52] and chemosensors [53-56]. The one-step synthesis of phenanthroimidazole derivatives has remarkably increased our own interest to involve a variety of aldehydes that may further extend the way for the introduction of other functionalities and to extend the conjugation for different purposes. The objective of designing a selective and sensitive dual anion responsive ratiometric probe has been achieved by developing a conjugated π-electron system containing specific ionophores, in which the electron rich phenanthroimidazole (the donor) and electron deficient dicyanovinyl (the acceptor) units are linked through a phenyl ring. The introduction of two distinct potential ionophores structurally, the -*N*H and dicyanovinyl units make sure **DCPPI** as an efficient dual anion sensing ICT probe which works on a push-pull mechanism of the donor and acceptor moieties in the present typical structural motif.

A simple three step synthetic route to afford **DCPPI** is shown in Scheme 1. Phenanthrene was first oxidized [67] by $K_2Cr_2O_7$ in aqueous-acidic medium to obtained 9,10-phenanthroquinone **2** in good yield (76%). Compound **2** upon reaction [45] with different aromatic aldehydes in the presence of ammonium acetate ($AcONH_4$) gave derivatives **3a-f** in 65%-80% yields. It is important to mention that **2** upon reaction with teraphthaldehyde gives mixture of products that were separated through column chromatography to obtain compound **3f** as a major product (~85%) and bis-phenanthroimidazolyl derivative **4** as a minor byproduct. Further, in order to introduce second ionophore unit aldehyde function of compound **3f** was reacted with malononitrile in the presence of triethylamine (TEA) to get 2,2–dicyanovinyl phenanthroimidazole, **DCPPI** as an orange color solid in 85% yield. The introduction of dicyanovinyl function makes **DCPPI** a suitable substrate to work as Michael acceptor which can easily undergo

nucleophilic addition reaction. As a proof of concept, potential probe **DCPPI** when treated with sodium cyanide in methanol gave tricyanophenanthroimidazolyl derivative, **DCPPIA** in good yield. The chemical structures were well characterized and data are given in supporting information (Figure–S1-S12).

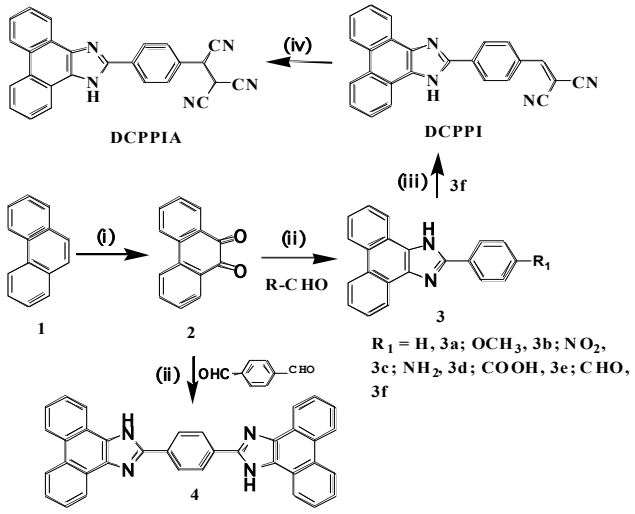

Scheme 1: (i) $K_2Cr_2O_7/H_2SO_4/\Delta$ (ii) R-CHO/$AcONH_4$/AcOH/Δ (iii) Malononitrile/DCM/TEA /r.t. (iv) NaCN/MeOH/r.t.

2.2. Colorimetric, UV-vis and Fluorescence Response

The sensor motif consisting of imidazole units are expected to interact with anions through hydrogen bonding interaction and/or deprotonation [1-6, 15-29]. Consequently, the change in intramolecular charge transfer (ICT) process will significantly affect the physicochemical behavior of the probe by push-pull mechanism [7-12, 19-29] and the color changes make the sensing event more sensitive, reliable and visible to the naked-eye. To strengthen our hypothesis we first observed the optoelectronic behavior of synthesized compounds in solvents of different polarity and data have been given in table-S1. The absorption and emission spectra of derivatives **3a-g** and **DCPPI** showed good solvatochromic behavior in which the absorption maxima, relative fluorescence intensity, Stoke's shift and color of the solution varied according to hydrogen bonding capabilities and polarities of solubilizing milieu [59] such as hexane, 1,4-dioxane, acetonitrile (MeCN), chloroform ($CHCl_3$), *N,N'*-dimethylformamide (DMF) and ethanol (EtOH) (Figure–1 and S13-13a). It is important to mention that hydrogen bonding between probe **DCPPI** and the solvents led to a bathochromic shift of the fluorescence maxima accompanied by increase in the Stoke's shift and molar absorbtivity. UV-vis absorption spectrum of **DCPPI** (5μM) in MeCN exhibited intramolecular charge transfer (ICT) band at 427 (ε = 2.99 x 10^4 M^{-1} cm^{-1}) while, the emission spectrum of **DCPPI** (1.5 μM) displayed emission at 614 nm ($\lambda_{ex.}$ at 427 nm; $\Phi_{\mathbf{DCPPI}}$ = 0.168; Stoke's shift (Δ) =7132 cm^{-1}) (Figure–2a,b).

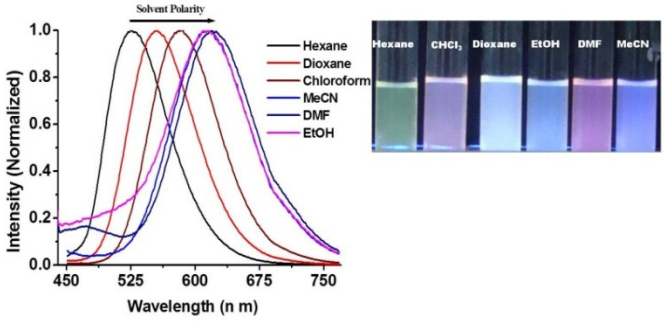

Figure 1: Normalized typical emission spectra and images (inset) of **DCPPI** in different medium.

2.3. Response of DCPPI toward anions in acetonitrile

It is important to mention that the non-covalent ionic recognition event of a receptor having amino and hydroxyl fragments as a potential ionophore are susceptible to interact with anions (like F- and AcO-) through hydrogen bonding interaction in solvents of variable polarity and are dependent on the basicity and structure aspects of the anions [15-29]. Therefore, the protic polar solvents should be avoided in anion recognition studies to substantiate actual mode of interaction [68-69]. While analyzing the photophysical behavior of different derivatives toward anion we found that acetonitrile (MeCN) is a suitable aprotic polar solvent because of ease in dissolving a wide range of ionic and nonpolar species, and easily miscible with water to create a homogeneous medium. Thus, considering the sensitivity of anions we intended to observe photophysical behavior of probe **DCPPI** toward different anions in MeCN.

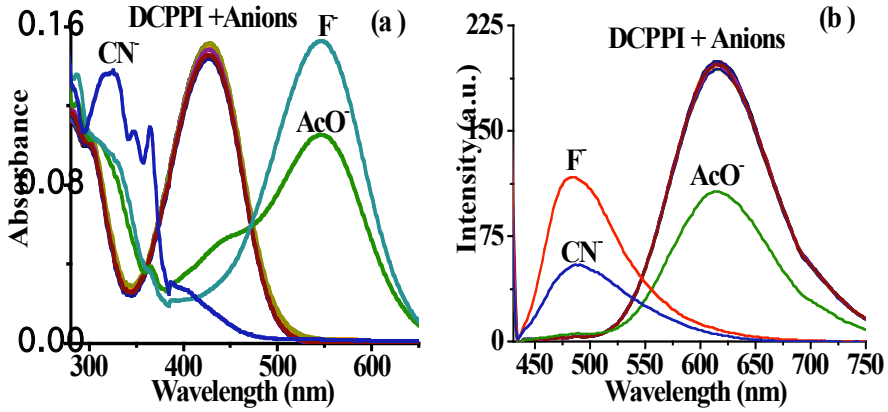

Figure 2: (a) Absorption (5 μM) and (b) Emission spectra (1 μM) of interaction of **DCPPI** with different anions (10 equiv) in MeCN.

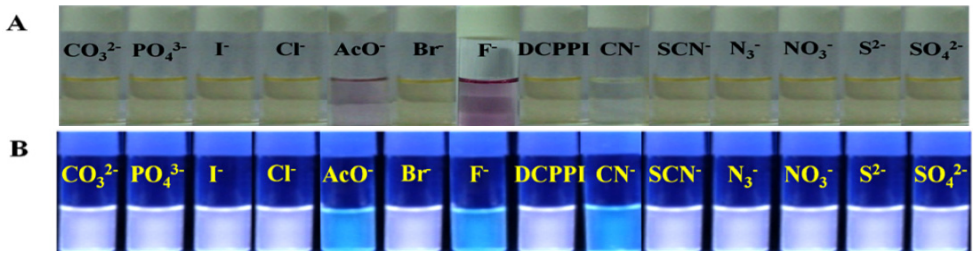

Figure 3: Images show change in color of **DCPPI** upon interaction with different anions (a) normal and (b) under UV light.

Notably, upon interaction with different class of anions (10 equiv) such as, F^-, Cl^-, Br^-, I^-, NO_3^-, N_3^-, SO_4^{2-}, $H_2PO_4^-$, CO_3^{2-}, AcO^-, CN^-, and SCN^- considerable change in the electronic transition spectrum of **DCPPI** was observed in the presence of F^-, AcO^- and CN^- ions. The ICT band centered at 427 nm disappeared and a new transition band appeared at 545 nm with F^- ($\varepsilon = 3.06 \times 10^4\ M^{-1}\ cm^{-1}$) and AcO^- ($\varepsilon = 2.11 \times 10^4\ M^{-1}\ cm^{-1}$) ions, respectively. Similarly, upon interaction with CN^- a blue shift of ~102-63 nm was observed and a new broad band appeared at 325 ($\varepsilon = 2.76 \times 10^4\ M^{-1}\ cm^{-1}$) with shoulders at 364 ($\varepsilon = 2.18 \times 10^4\ M^{-1}\ cm^{-1}$), and 347 ($\varepsilon = 2.15 \times 10^4\ M^{-1}\ cm^{-1}$) nm (Figure–2a). Moreover, upon interaction with different tested anions the emission intensity of **DCPPI** (at 614 nm; $\lambda_{ex.}$= 427 nm; 1 μM) showed partial fluorescence quenching (~ 46%) with AcO^- whereas, with F^- and CN^- emission band centered, at 614 nm disappeared completely and new emission bands appeared at 492 and 490 nm (blue shift, ~122 and 124 nm) respectively (Figure–2b). The spectral pattern observed in the presence of F^- and AcO^- suggested about the probability of deprotonation and/or H-bonding with the ionophore, the –*N*H fragment of **DCPPI**. Similarly, upon interaction with CN^- the variation observed in the emission and absorption spectra suggested about the possibility of formation of new stable species in the medium. Additionally, colorimetric naked eye sensitive light yellow-green color solution of **DCPPI** changed to a light pink with F^- (stable for almost 24 hr) and AcO^- (stable for ~10 min) while with CN^- a transient red-pink color disappeared within second to become colorless. However, under UV light considerable fluorogenic response observed wherein, a stable fluorescent white-blue color of **DCPPI** appeared as light blue, immediately upon interaction with F^-, AcO^- and CN^- ions (Figure–3). The other tested anions failed to exhibit any significant change in the absorption and emission spectra.

2.4. Response of DCPPI in Aqueous medium:

Furthermore, to our own interest we attempted to understand the optical behavior of **DCPPI** toward anions in partial aqueous medium. This is because in aqueous or semiaqueous medium, salvation energy [57,58] for CN^- remains low (ΔH_{hyd} = -67 kJ/mol) in comparison to other anions (for example; ΔH_{hyd} = -505, -363, -336, -295, -375, -260, kJ/mol for F^-, Cl^-, Br^-, I^-, AcO^-, and $H_2PO_4^-$ respectively in H_2O/MeCN)

and would enhance selectivity of **DCPPI** for CN^-.The absorption spectrum of **DCPPI** (5 μM) in H_2O-MeCN (50%) showed ICT band at 423 (ε = 2.26 x 10^4 M^{-1} cm^{-1}) nm and exhibited emission toward high wavelength, at 634 nm (at λex. = 423 nm). Interestingly, when we examined the probe in the presence of different tested anions (20 equiv) **DCPPI** showed high selectivity for CN^- in which ICT band centered, at 423 nm disappeared and new broad band appeared at 363 (ε = 1.70 x 10^4 M^{-1} cm^{-1}), 345 (ε = 1.50 x 10^4 M^{-1} cm^{-1}) and 325 nm (ε = 1.64 x 10^4 M^{-1} cm^{-1}) (Figure–4a). Similarly, the emission spectrum of **DCPPI** (1 μM) displayed significant fluorescence quenching (at 634 nm) only with CN^- and a new emission band appeared at 514 nm (blue shift, ~120 nm) (Figure–4b). The significant blue shift in the emission behavior of **DCPPI** could be attributed to a possible Michael type nucleophilic addition reaction, leading to the formation of a Michael adduct in the medium. However, rest of the anions failed to exhibit any significant change in the transition spectra. Interference studies have been performed by the addition of excess of competitive anions (40 equiv) to a probable solution of **DCPPI+CN^-**. The observed insignificant change in the absorption and emission spectra of **DCPPI+CN^-** (Figure–S14) make sure high selective affinity of **DCPPI** for cyanide anion.

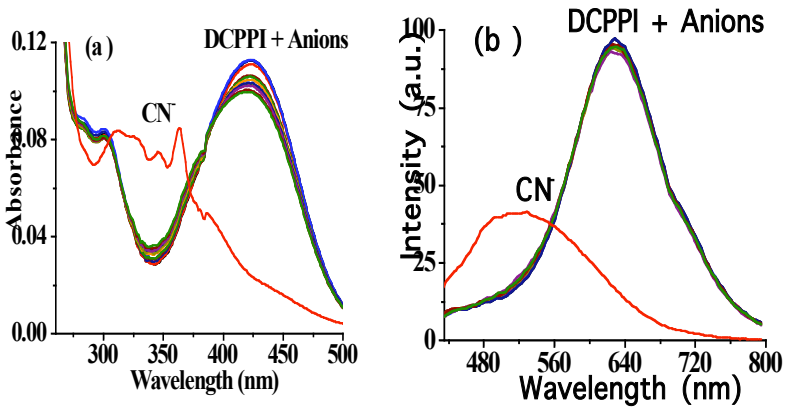

Figure 4: (a) Absorption (5μM) and (b) Emission spectra (1μM) of **DCPPI** upon interaction with different anions (20 equiv) in H_2O-MeCN (50 %).

2.5. Binding Affinities of DCPPI toward different Anions

The binding affinities of **DCPPI** (5 μM) toward tested anions have been examined through the absorption and emission titration experiments in acetonitrile (Figure–5). Upon a sequential addition of F^- (0-9 equiv) the ICT band centered, at 427 nm reduced gradually and a new absorption band appeared at 545 nm, ratiometrically. The formation of an isosbestic point at 470 nm suggested the existence of more than one species in the medium (Figure–5a). Similarly, the emission titration experiment was performed by the addition of F^- (0-30 equiv.) ion to a solution of **DCPPI**. The emission intensity of **DCPPI** centered, at 614 nm diminished gradually and a new emission band with enhanced relative fluorescence intensity appeared at 492 nm, ratiometrically (Figure–5b). A careful examination of emission titration spectra suggested that

upon addition of ~10 equiv of F^- initially, the relative emission intensity, at 614 nm quenched significantly with decrease in quantum yield (~65%; $\Phi_{DCPPI+F^-} = 0.058$). Further, addition of F^- ions (10 to 30 equiv.) led to significant increase in emission intensity of a new emission band, at 492 nm, and the net quantum yield enhanced by ~74% ($\Phi_{DCPPI+F^-} = 0.223$). The observed significant change in the emission spectra suggested about the deprotonation of N–H fragment of **DCPPI.** Consequently, ICT increases due to charge propagation form phenanthroimidazolyl unit to electron deficient dicyanovinyl fragment. Job's plots analysis revealed a 1:1 stoichiometry for a probe-fluoride interaction, consistently. The binding constants based on absorption and emission titration spectral data have been estimated through Benesi-Hildebrand (B-H) method [70,71], and were found to be K_{ass}(abs) = 2.96 x 10^4 /M and K_{ass}(em) = 3.82 x 10^4 /M respectively (Figure–5c, S15a, and Table–1).

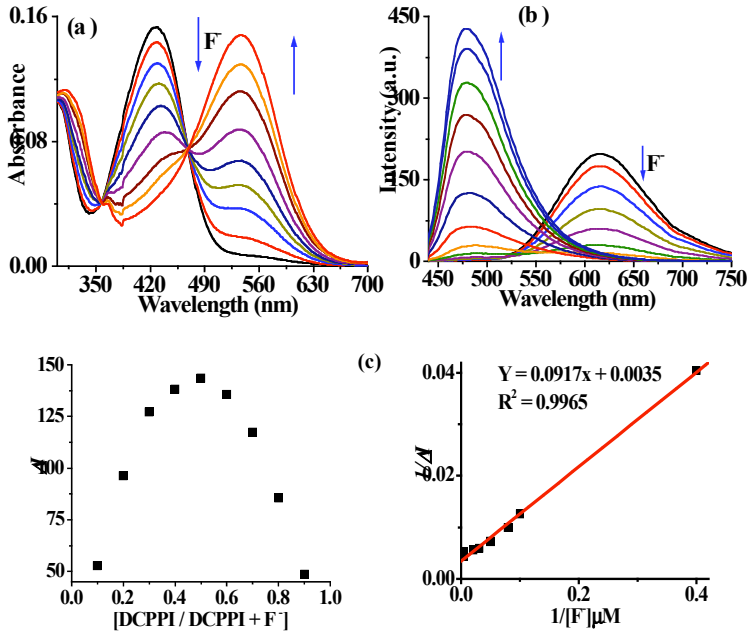

Figure 5: (a) Absorption (5μM) and (b) emission (1.5μM) titration spectra of **DCPPI** upon addition of (0-9 equiv) and (0-30 equiv) of F^- anions, respectively in MeCN. (c) Job's plot and Benesi-Hildebrand plots obtained from emission spectral data.

Similarly, the absorption titration spectra of **DCPPI**, revealed almost similar spectral pattern in the presence of AcO^- (0–7 equiv) ions in which, ICT band (at 427 nm) disappeared and a new band appeared at 545 nm, concomitantly (Figure–S15a,b). Moreover, the emission spectra upon addition of AcO^- (0-35 equiv.) displayed ratiometric behavior in which the emission intensity (at 614 nm) diminished completely, along with decrease in quantum yield by ~58% ($\Phi_{DCPPI+AcO^-} = 0.07$) and a new emission band appeared at 486 nm ($\Phi_{DCPPI+AcO^-} = 0.083$). The formation of isosbestic and isoemissive points at 475 and 548 nm, respectively, further suggested about the presence of more than one species in the medium. Job's plots analysis revealed a 2:1 equilibrium for an interaction between **DCPPI** and AcO^- for which binding constant

has been estimated using emission titration data and were found to be 1.48 x 10^2 /M (Figure–S15c, d, Table–1).

Further to understand the binding behavior of cyanide both absorption and emission titration experiments were performed. The typical spectral changes that occur for **DCPPI** as a function of CN^- are shown in Figure 6. As can be seen in Figure 6a, the intensity of ICT band (at 427 nm) decreased upon a gradual addition of 0–2 equiv. of CN^- and a new band appeared at 545 nm (ε = 1.25 x 10^4 $M^{-1}cm^{-1}$). However, further addition of CN^- (2 to 5.0 equiv) decrease the absorption of new band, (at 545 nm) and high energy band appeared at 331-361 nm, progressively and the color of solution disappeared. More interestingly, the emission spectrum of **DCPPI** upon addition of 0-4 equiv. of CN^- showed significant fluorescence quenching in which relative emission intensity (centered, at 614 nm) decreased, ~ 90% (Figure–6b) along with decrease in quantum yield by ~60% ($\Phi_{DCPPI+CN^-}$ = 0.069). A further addition of CN^- (4.5-14 equiv) led to successive fluorescence enhancement at 490 nm and the quantum yield increased by 50% (~2 fold; $\Phi_{DCPPI+CN^-}$ = 0.14).

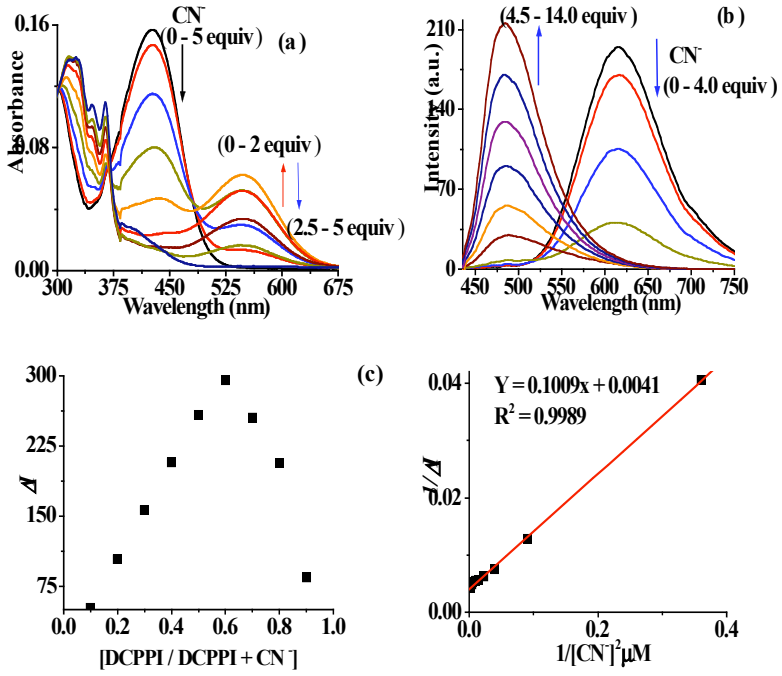

Figure 6: (a) UV-vis absorption (5μM) and (b) emission titration spectra (1.5μM) of **DCPPI** upon addition of 0-5 equiv and 0-14 equiv of CN^- in MeCN. (c) Job's plot and Benesi-Hildebrand plots obtained from emission spectral data.

The color of solution became light blue with saturation in emission spectral profile (Figure–6b and 3b). It is interesting to mention that interaction of **DCPPI** with CN^- led to existence of two successive reaction equilibria in the medium. The stoichiometry for the possible mode of interaction between **DCPPI** and CN^- has been realized. Job's plot analysis revealed a 1:1 equilibrium at low concentration of CN^-. However, as the concentration of CN^- increased equilibrium changed to 1:2 from 1:1. The binding constants for a 1:2

equilibrium have been estimated through the nonlinear fittings of titration data and were found to be $K_{ass(abs)}$ = 1.5 x 10^{10} /M^2 and $K_{ass(em)}$ = 4.06 x 10^{10} /M^2 respectively (Figure–6c, S16b, and Table–1). Thus, the significant change in the physicochemical properties of **DCPPI** clearly suggested about the interaction of CN^- through different channels and in two successive steps. First, ICT get restricted, due to the formation of a Michael adduct, **DCPPI**-CN^- and fluorescence quenching observed at 614 nm. Secondly, the interaction of CN^- with second ionophore, the –*N*H fragment of resultant adduct, **DCPPI**-CN^- led to enhance ICT due to an increase in charge density on the phenanthroimidazolyl unit, that finally led to a significant fluorescence enhancement (at 490 nm) [19-29, 50-58].

Moreover, since the changes in optoelectronic behavior of probe in the presence of different anions so rapid it was difficult to obtain a precise kinetic plot. We tried to obtain kinetic plot by the addition of CN^- (~20 equiv) to a solution of **DCPPI** and measured the emission spectra at regular time interval. A time versus relative fluorescence intensity plot has indicated about the completion of reaction and the changes in photophysical properties of the probe approximately within ~ 10 min, wherein the intensity of emission band, centered at 614 nm decrease gradually while the intensity of a new emission band (appeared at ~490 nm) enhances ratiometrically (Figure–S17).

Table – 1: Estimated data for probe **DCPPI**.

Entry	ε (10^4 M^{-1} cm^{-1}) / λ (nm)	λem (nm)/(Φ) Quantum yield	Binding constant			Limit of Detection (LOD)
			Stoichiometry	K_{ass} (abs)	K_{ass} (em)	
DCPPI	2.99 (427)	614/(0.168)				
DCPPI + F^-	3.06 (545)	614/(0.058) 492/(0.223)	1:1	2.96 x 10^4 /M	3.82 x 10^4 /M	149 nM (~2.83 ppb)
DCPPI + AcO^-	2.11(545)	614/(0.070) 486/(0.083)	2:1	--	1.48 x 10^2 /M	
DCPPI + CN^-	2.15 (325); 2.76 (364)	614/(0.069) 490/(0.14)	1:2	1.5 x 10^{10} /M^2	4.06 x 10^{10} /M^2	210 nM (~5.5 ppb)

2.6. Limit of Detection (LOD) for DCPPI with different anions

The limit of detection (LOD) for F^- and CN^- ions have been estimated through the fluorescence spectroscopic method, as reported previously [59-66]. A calibration curve was obtained by measuring the fluorescence spectra of different concentration (from 5.2 μM to 0.8 μM) of **DCPPI**. An approximately straight calibration curve suggested about a linear correlation between relative fluorescence intensities and

concentrations of the probe and gave standard deviation (σ) 0.30 as a function of probe concentrations (Figure–S18a). To estimate calibration sensitivity (m) fluorescence plots between ΔI ($I - I_0$) (where I_0 and I illustrate the emission intensities of **DCPPI** in the presence and absence of F^- and CN^- ions respectively) and concentration of both the anions (F^- / CN^-) were obtained in the aforementioned range (Figure–S18b,c). The slope of fluorescence curves gave calibration sensitivity (*m)* 6.03 and 4.27 for F^- and CN^-, respectively. Now, equation (4) has been utilized to obtain the limit of detection (LOD) for F^- and CN^- ions as 149 nM (2.83 ppb) and 210 nM (5.5 ppb), respectively (Table–1). Thus, the **DCPPI** can be applied to detect F^- and CN^- in *nM* range which might fulfill the requirement of a potential fluorescent chemosensor and chemodosimeter to sense anions in drinking water as well as in biosensing [72].

2.7. Nature of Interaction between DCPPI and F^-/CN^- ions

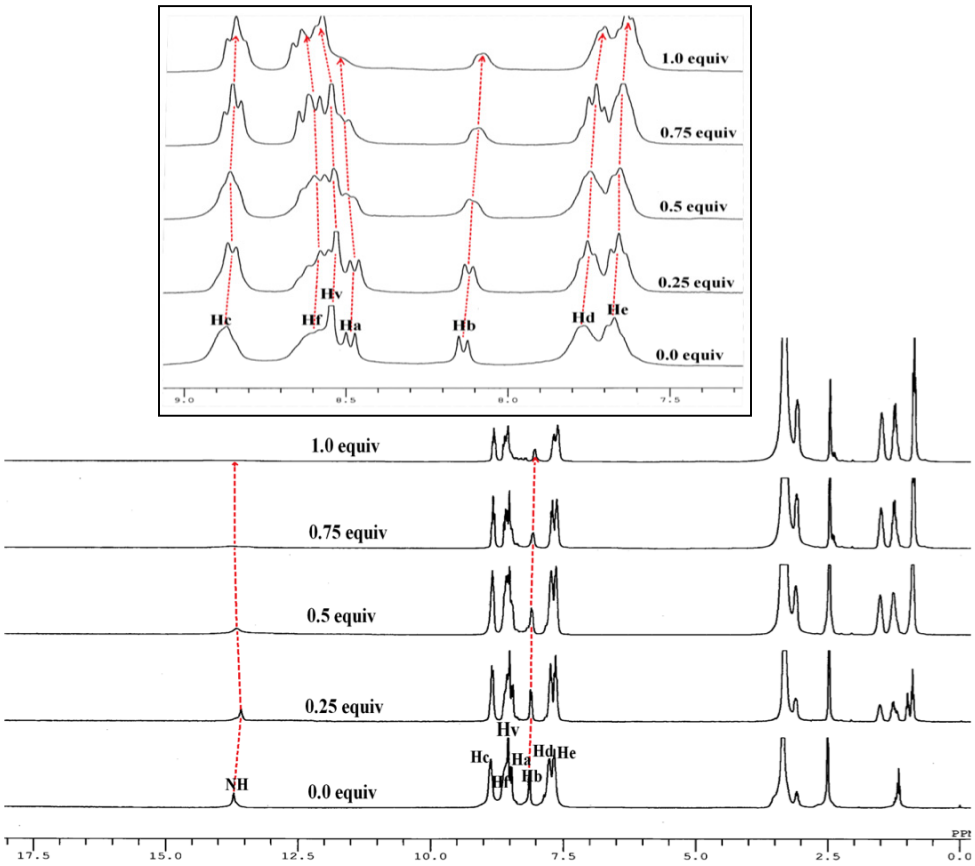

Figure 7: Stacked ^{1}H NMR spectra of **DCPPI** (2.1 x 10^{-2} M) upon addition of F^- ions (0-1.0 equiv) in DMSO-d_6.

To gain further insight into the actual nature of interaction ^{1}H NMR titration experiments were performed. The ^{1}H NMR spectrum of **DCPPI** (2.1 x 10^{-2} M; DMSO-d_6) (Figure–7) showed doublet(s) at δ 8.495-8.467(J = 8.4 Hz), 8.152-8.124 (J = 8.4 Hz), 8.863-8.842 (J = 6.3 Hz) and 8.577-8.552 (J = 7.5 Hz) ppm corresponding to H*a*, H*b*, H*c*, and H*f* resonances, respectively. A multiplet appeared at δ 7.76-7.66 ppm

may be assigned to resonances of H*d* and H*e* protons (Figure–7, S5) while resonances appeared at δ 13.713 and at δ 8.53 ppm, respectively are attributable to -*N*H and H_V protons of imidazolyl and dicyanovinyl units. Upon a sequential addition of F^- ions (0-1.0 equiv) to a solution of **DCPPI** the -*NH* resonance initially broadened and disappeared. The chemical shifts corresponding to resonances of H*c*, H*b* and H*d*, H*e* protons shifted upfield and appeared at δ 8.84 (Δδ = 0.023 ppm), 8.06 (Δδ = 0.086 ppm), and 7.69 (Δδ = 0.063 ppm) ppm. Similarly, significant downfield shifts corresponding to H*f* (8.664; Δδ = 0.087 ppm), H_V (8.573; Δδ = 0.043 ppm) and H*a* (8.637; Δδ = 0.142 ppm) proton resonances were also observed (Figure–S19-22). Thus, the observed noticeable change particularly, at the –NH proton of **DCPPI** suggested about the deprotonation of the N–H fragment in the presence of F^- [19-29].

Similarly, the ^{1}HNMR titration spectra (Figure–8) of **DCPPI** illustrated significant changes in the presence of CN^- ions. Upon addition of 0.25 to 0.5 equiv of CN^- chemical shift corresponding to H_V proton (at δ 8.53 ppm) get reduced and a new signal (H_V') appeared in the high field region, at δ 4.687 ppm. Further after addition of 1.0 equiv of CN^- H_V signal disappeared completely and $H_{V'}$ signal dominated. Simultaneously, after addition of 0.5 equiv of CN^- the -*N*H proton signal (at δ 13.713 ppm) broadened without any significant shift and disappeared completely after the addition of 0.75 equiv of CN^-. The other observed change in the ^{1}H NMR signals was almost consistent to changes occurred with F^- ions. Moreover, the resonances attributed to H*c*, H*d* and H*e* protons shifted upfield to appear at δ 8.83 (Δδ = 0.03 ppm) and δ 7.715 (Δδ = 0.045 ppm) ppm while H*b*, H*f* and H*a* protons shifted downfield to appear at δ 8.302(Δδ = 0.15 ppm) and 8.628(Δδ = 0.05 ppm) ppm, respectively (Figure–8, S23-25). Thus, clearly suggested about the dual mode of interaction wherein, first Michael adduct was formed due to nucleophile addition of cyanide at the dicyanovinyl fragment. The new entity so formed then further establish an interaction with -NH fragment of phenanthroimidazolyl [35,26] through the -N…CN…H type of hydrogen bonding leading to typical deprotonation of the N–H function [19-29].

Further to prove the interaction of **DCPPI** with cyanide ^{13}C NMR spectra were analyzed. In the absence of cyanide ^{13}C NMR spectrum of **DCPPI** showed resonances at δ 160.24, 148.67, 147.389, 137.730, 113.56 and 112.33, and 80.98 ppm attributable to C3, C8, C7, C4, C1 and C2 carbons, respectively (Figure–S6). Upon addition of 1.5 equiv of CN^- the C3, C2 and C7 carbon signals shifted considerably in the upfield region and appeared at δ 30.344, 25.473 and 143.33 ppm, respectively while the C8 signal shifted downfield to appear at 148.792 ppm. Moreover, the carbon resonances of the phenyl ring showed upfield shift and was in the range of Δδ 0.15 to 3 ppm (Figure–S26). The significant upfield shift in the resonances of C2 and C3 carbons clearly supported the formation of a Michael types adduct, **DCPPI**-CN^- in the medium. Simultaneously, the downfield shift occurred in the resonances of C8 carbon also suggested about the interaction of CN^- with –*N*H fragment of the imidazolyl unit through the hydrogen bonding [19-29].

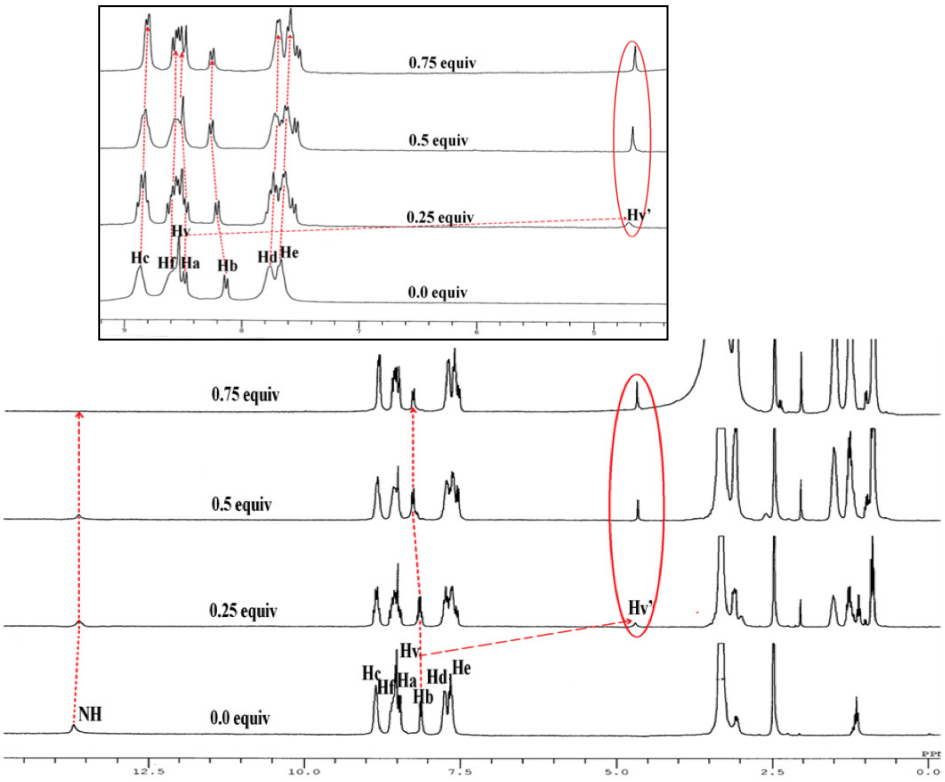

Figure 8: Stacked ^{1}H NMR spectra of **DCPPI** (2.1 x 10^{-2} M) upon addition of CN^- ions (0-0.75 equiv.) in DMSO-d_6. Inset: partial stacked ^{1}HNMR spectra.

It is worth to mention that both F^- and CN^- ions have enough basicity to act as proton abstractors. When both the anions come close to the N–H fragment (acidic in nature) of phenanthroimidazolyl unit hydrogen bonding interaction occurs in the early transition state, which leads to a partial proton transfer from the probe to anions. Later on, the net increase in charge density, due to deprotonation of NH unit, causes shielding effect and leads to a significant change in the photophysical behavior of the probe along with change in the color of solution. Additionally, 1:1 and 1:2 stoichiometries evidenced different mode of interaction between **DCPPI** and F^- and CN^- ions, respectively. The photophysical and NMR spectral behavior clearly suggested that CN^- first reacted with dicyanovinyl function of **DCPPI** to form a Michael type adduct, **DCPPI**-CN^-, and restrict the ICT. Consequently, the emission intensity of the probe, centered at 614 nm decreased significantly due to hindrance in relay of CT from electron rich phenanthroimidazolyl ring to electron deficient/withdrawing dicyanovinyl unit of **DCPPI**. The same rationale has been taken into account to describe the changes in the electronic transition spectra of **DCPPI**. Therefore, **DCPPI** can also be termed as a chemodosimeter to detect cyanide anion.

Moreover, upon increasing the concentration of CN^- to a solution of **DCPPI** a new emission band with enhanced fluorescence intensity appeared at 490 nm due to hydrogen bonding interaction and/or deprotonation between CN^- and –*N*H fragment. Interestingly, almost similar pattern was observed when F^-

interacted with **DCPPI**. Thus, on the basis of changes in optical properties of the **DCPPI** it is worth to infer that both anions are capable to induce deprotonation of N–H fragment [19-29]. However, in case of cyanide the resultant increase of charge density remained delocalized to the phenanthroimidazolyl unit and the enhanced ICT mainly centered at the newly formed anionic species. Thus, the net CT gets restricted and could not propagate to reach up to cyano terminal. As a consequence, ICT become restricted and led to a considerable blue shift in the absorption and emission bands along with enhancement in relatively emission intensity. A plausible mechanism for interaction of **DCPPI** with both the anions has been shown in scheme–2.

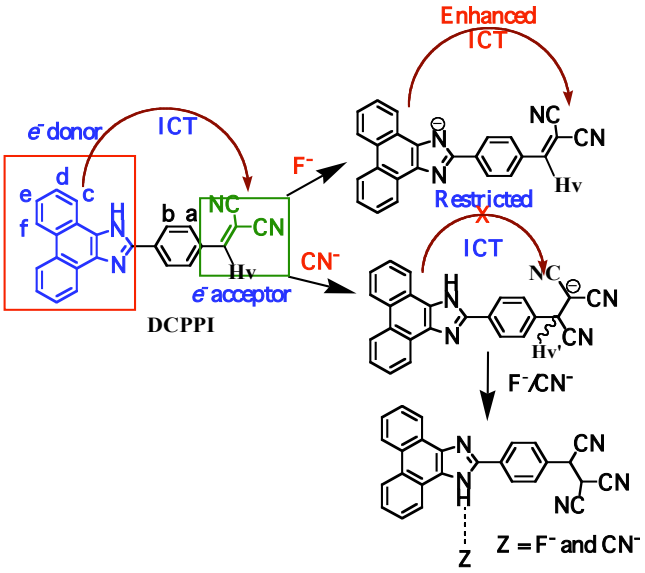

Scheme -2: Proposed mechanism of interaction for **DCPPI** in the presence of F^- and CN^- ions.

2.8. Theoretical Calculations

Furthermore, variation in the optical behavior of **DCPPI** has also been correlated theoretically by density functional theory (DFT) calculation method. The DFT optimization using B3LYP/6-31G* level [73] revealed a planer structure of **DCPPI** with extended π-conjugation between phenanthroimidazolyl and dicyanovinyl units. The imidazole ring of **DCPPI** shows bond distances ~1.32 and 1.38 Å with an angle 111^0 for N-C-N- unit. The bond length between dicyanovinyl group and phenyl ring appeared around 1.44 to 1.39 Å with an angle 131^0. Due to deprotonation of the -*N*H unit by F^- ion the bond length of imidazolyl ring changed to 1.36 Å with an angle 116^0. Thus, suggesting about delocalization of charge on the imidazolyl ring. Whereas, upon interaction with CN^- bond length between phenyl and dicyanovinyl unit increased to 1.54-1.52 Å with an angle of 115^0 possibly due to formation of **DCPPI**-CN^- adduct while, the imidazolyl ring remained unaffected (Figure–9a).

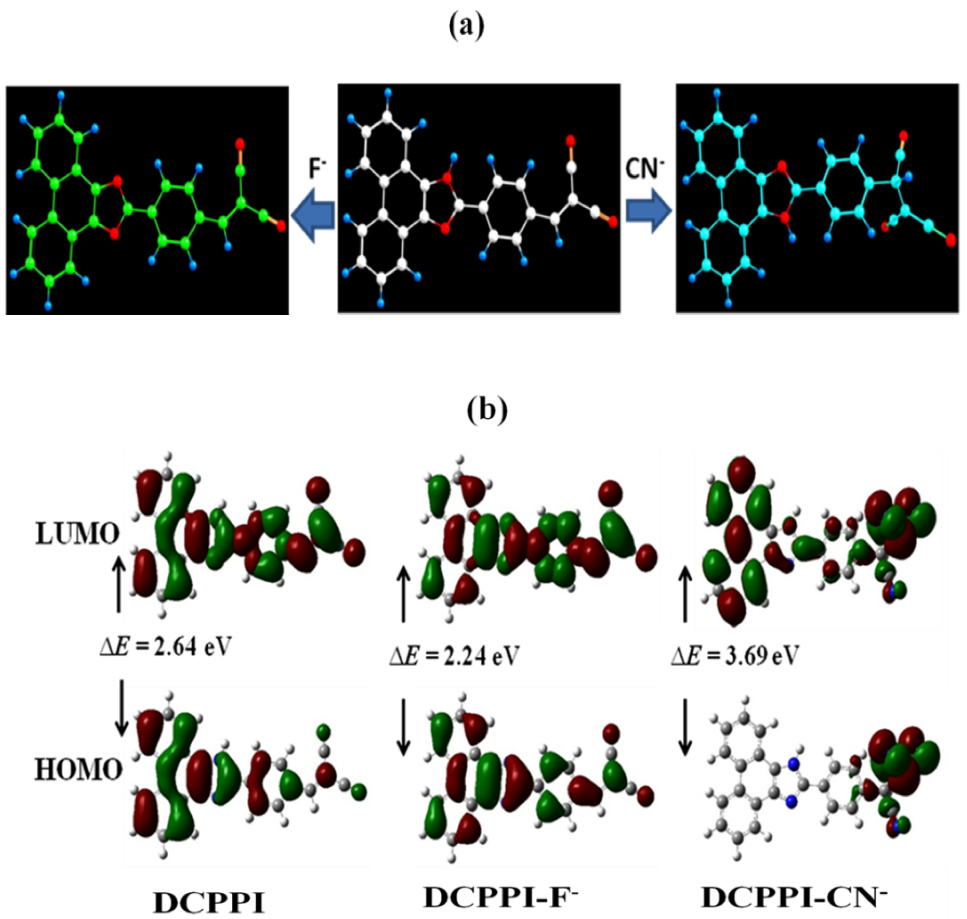

Figure 9: (a) DFT optimized structures and (b) Molecular Orbitals for **DCPPI**, **DCPPI**-F^- and **DCPPI**-CN^- .

The molecular orbital pictures indicate that the HOMO is localized on phenanthroimidazolyl unit while LUMO on **DCPPI** thus, the possibility for ICT between phenanthroimidazolyl to dicyanovinyl unit is reasonable to understand (Figure–9b). After -*N*H deprotonation by F^- the HOMO and LUMO reorganized to localize over entire molecule. Consequently, a decrease in the energy gap between HOMO and LUMO corroborate well with the enhanced ICT and fluorescence. Similarly, as **DCPPI**-CN^- adduct is formed the HOMO and LUMO become localized and delocalized at dicyano unit and on entire adduct, respectively. As a consequence, ICT between the phenanthroimidazolyl and dicyanovinyl units get restricted because of hindrance in extended π–conjugation and led to a blue shift in emission spectra which is well supported by the increase in energy gap between the HOMO and LUMO.

3. Synthesis and characterization of DCPPI-CN^- adduct, DCPPIA.

In order to confirm the feasibility of a Michael type nucleophilic addition reaction between **DCPPI** and CN^- adduct **DCPPIA** was prepared (Scheme – 1) by reacting **DCPPI** with NaCN in methanol. The compound was isolated and characterized by spectral data analysis (Figure S9–12). The ^{1}H NMR spectrum

of **DCPPIA** in DMSO-d_6 showed resonances as triplet, multiplet and doublet attributable to H_c, H_f, H_d H_e, and H_a, H_b, protons at δ 8.89 (*t*, J_1 = 8.7 Hz, J_2 = 7.8 Hz), 8.60 (*t*, J_1 = 7.8 Hz, J_2 = 8.7 Hz), 7.76-7.65 (*m*) and 8.47 (*d*, *J* = 8.4 Hz), 8.19 (*d*, *J* = 8.1 Hz) ppm, respectively. A broad and sharp singlet appeared at δ 13.68, 4.07 and δ 3.91 ppm may be assigned to –*N*H, H_{V}' and H_{V}'' resonances of imidazolyl ring and aliphatic protons, respectively (Figure–S9). The ^{13}C NMR spectrum of **DCPPI** showed resonances at δ 160.24, 148.67, 147.389, 137.730, 113.56 & 112.33, and 80.98 ppm probably due to C3, C8, C7, C4, C1 and C2 carbons, respectively (Figure–S6). In contrast, in the ^{13}C NMR spectrum of **DCPPIA** the signal attributable to C3 carbon disappeared and new signals appeared at δ 29.033, 23.701 and 113.797 ppm (Figure–S10). These signals could be assigned to new aliphatic carbons (C3' and C2') and a new cyanocarbon (C1") introduced in adduct, **DCPPIA**. Moreover, the FT-IR spectrum of **DCPPI** has shown probable stretching vibration bands attributable to N-H, C≡N, C=C and aromatic C=C, C-H functions at 3378, 2229, 1689, and 1655 1606 1579 1455 1427 1236 1163 cm^{-1} (Figure–S7). In contrast, **DCPPIA** illustrated probable N-H, aliphatic C-H, C≡N, and aromatic C=C, C-H stretching vibration bands at 3339, 2923 2853, 2194 and 1656 1614 1551 1456 1426 1235 1111 cm^{-1} (Figure–S11). Typically, for **DCPPIA** the C=C stretching vibration band disappeared and two new aliphatic C-H stretching vibrations bands appeared at 2923, 2853 cm^{-1}. The ESI-MS spectral data analysis of **DCPPI** showed a molecular ion $[DCPPI+2H]^+$ peak at m/z 372.3 whereas in case of **DCPPIA** molecular ion $[DCPPIA+H]^+$ peak appeared at m/z 398.3. Moreover, HRMS (ESI-TOF) shows molecular ion peak, m/z: for $[DCPPI + H]^+$ ($C_{25}H_{14}N_4$ calc. 371.1291; Found 371.1292) and for $[DCPPIA + H]^+$ ($C_{26}H_{15}N_5$ calc. 398.1403; Found 398.1402) (Figure–S8, 12). Thus, the spectral data analysis altogether supported the formation of Michael adduct in the medium**.**

Conclusion

In summary, we have developed an efficient donor-acceptor type intramolecular charge transfer (ICT) probe and describe its photophysical behavior in different medium. Owing to presence of appreciably acidic imidazolyl NH fragment the probe has been utilized for multichannel recognition of F^- and CN^- ions. The anion sensing studies have been studied by absorption, emission and NMR spectroscopy. The observations made from the physicochemical studies unequivocally suggested about the successive deprotonation of potential fluoroionophore, the NH fragment present on the phenanthroimidazolyl unit, in the presence of F^- and CN^- ions. The experimental and theoretical observations altogether supported the proposed mechanism of sensing via different channels. The multichannel recognition of cyanide in two successive steps is well supported by spectral behavior of **DCPPI** and its adduct **DCPPIA** in which ICT get restricted initially due to the formation of Michael type adduct, **DCPPIA** and then the interaction of cyanide with –*N*H fragment of imidazolyl unit enhances ICT due to an increase in charge density on the phenanthroimidazolyl unit consequently, led to a significant fluorescence enhancement.

Experimental Section

Synthesis of probe DCPPI

(1) Synthesis of 1,10-phenanthroquinone 2: To a solution of H_2SO_4/H_2O (20 ml:60 ml, v/v), phenanthrene (2 g, 11.23 mmol) was added and the reaction mixture was stirred at 90-95^oC for 4 h. $K_2Cr_2O_7$ (12 g) was added in parts to the reaction mixture for 1 h and heated for 30 min. After complete reaction (monitored on TLC), cold water (200 ml) was added and precipitate so obtained was filtered, washed with water (3x50 ml). The precipitate was suspended in ethanol (60 ml) and saturated solution of sodium metabisulfite (30 ml) was added with frequent stirring for 15 min. Further, water (150 ml) was added to the reaction mixture to dissolve the product and filtered. To the filtrate Na_2CO_3 solution (20%, 50 ml) was added to decompose adduct and allowed it to precipitate. The precipitate was filtered, washed with water and dried in air to obtain orange colored solid. The product was recrystallized from glacial acetic acid. Yield 76% (1.77 g). M p: 209 ^oC. R_f = 0.7 ($CHCl_3$); ^1H NMR ($CDCl_3$) δ (ppm): 8.20 (d, 2H, *J* = 7.5 Hz), 8.03 (d, 2H, *J* = 8.1 Hz), 7.74 (t, 2H, *J* = 7.2, 7.2 Hz), 7.49 (t, 2H, *J* = 7.5, 7.5 Hz); FT-IR (KBr) υ_{max} (cm^{-1}) 1676, 1594, 1451, 1478, 1334, 1284, 1230, 925, 760, 533, 434.

(2) Synthesis of imidazole 3a-f and 4: To a solution of **2** (1 mmol) in acetic acid (15 ml), aromatic aldehydes (1 mmol) and $AcONH_4$ (308 mg, 4 mmol) were added. The reaction mixture was refluxed for 2-3 h and monitored (on TLC). The reaction mixture was allowed to cool at room temperature and poured in to water (30 ml). The precipitate so obtained was filtered, washed with acetic acid and water (3 x 5 ml). The crude products were purified through silica gel column to afford compounds in good yield.

3a: Yield 62%, Mp: 315-318 ^oC, ^1H NMR (300 MHz, DMSO-d_6) δ (ppm): 13.53 (s, 1H, NH), 8.87 (m, 2H), 8.56-8.51 (m, 2H), 8.32-8.31 (d, 2H, *J* = 7.5 Hz), 7.65-7.59 (m, 4H), 7.50(t, 1H, *J* = 7.5 Hz).

3b: Yield 60%, Mp: > 300^oC, ^1H NMR (300 MHz, DMSO-d_6) δ (ppm): 13.28 (s, 1H, NH), 8.84-8.83 (d, 2H, *J* =7.3 Hz), 8.57-8.54 (d, 2H, *J* = 7.5 Hz), 8.25-8.22 (d, 2H, *J* = 8.7 Hz), 7.72-7.61 (m, 4H), 7.17-7.14(d, 2H, *J* = 8.4 Hz, 3.85 (s, 3H, $-OCH_3$).

3c: Yield 65%, Mp: > 300^oC, ^1H NMR (300 MHz, DMSO-d_6) δ (ppm): 13.83 (s, 1H, NH), 8.87-8.86(d, 2H, *J* = 7.2 Hz), 8.56-8.53 (m, 4H), 8.47-8.44 (d, 2H, *J* = 9.0 Hz), 7.73-7.67 (m, 4H).

3d: Yield 55%. Mp: > 300^oC, ^1H NMR (300 MHz, $CDCl_3$) δ (ppm): 8.66-8.64(d, 2H, *J* = 7.8 Hz), 8.32 (1H, broad, NH) 7.87-7.85 (d, 2H, *J* = 8.1 Hz), 7.59-7.53 (m, 6H), 6.70-6.68 (d, 2H, *J* = 7.8 Hz), 3.82(broad, $-NH_2$).

3e: Yield 70%, Mp: > 300^oC, ^1H NMR (300 MHz, DMSO-d_6) δ (ppm): 13.66 (s, 1H, NH), 13.15(1H, broad, -COOH), 8.875 (m, 2H), 8.58 (m, 2H), 8.44-8.41 (d, 2H, *J* = 8.1 Hz), 8.17-8.14 (d, 2H, *J* = 8.1 Hz), 7.75-7.66 (m, 4H).

3f: Yield 65% (0.27 g). Mp: 311^oC. R_f = 0.5 ($CHCl_3$); ^1H NMR ($CDCl_3$) δ (ppm): 9.77 (s, 1H), 8.66 (d, 2H, *J* = 6.6 Hz), 8.34 (d, 2H, *J* = 8.7 Hz), 8.09 (d, 2H, *J* = 8.1 Hz), 7.66 (m, 6H); FT-IR (KBr) υ_{max} (cm^{-1}) 3379, 2923, 1690, 1602, 1455, 1428, 1307, 1212, 1163, 836, 755, 722.

4: Yield 82%, Mp: > 300^{o}C, ^{1}H NMR (300 MHz, DMSO-d_6) δ (ppm): 13.65 (s, 2H, NH), 8.89-8.86 (d, 2H, J = 8.1 Hz), 8.86-8.83 (d, 2H, J = 8.3 Hz), 8.66-8.64 (d, 2H, J = 7.5 Hz), 8.63-8.60 (d, 2H, J = 8.0 Hz), 8.54 (s, 4H), 7.85-7.79 (m, 4H), 7.71-7.65(m, 4H,).

(3) Synthesis of probe DCPPI: To a solution of **3f** (0.16 g, 0.5 mmol) in DCM (10 ml), malononitrile (38 mg, 0.6 mmol) and catalytic amount of triethylamine (TEA) (0.5 ml, 0.36 mmol) were added. The reaction mixture was stirred overnight at room temperature. The precipitate obtained was filtered and washed with DCM and dried in air to get the **DCPPI** as an orange-red colored solid. The compound was reconstituted in acetone and purified by silica gel column chromatography using gradient of hexane and ethyl acetate (v/v 70/30). Yield 85% (0.158g). Mp: 336-339 ^{o}C. R_f = 0.6 ($CHCl_3$); ^{1}H NMR (300 MHz, DMSO-d_6) δ (ppm): 13.713 (1H, broad, NH), 8.863-8.842 (d, 2H, J = 6.3 Hz), 8.577-8.552 (d, 2H, J = 7.5 Hz), 8.53 (s, 1H, Hv), 8.495-8.467 (d, 2H, J = 8.4 Hz), 8.152-8.124 (d, 2H, J = 8.4 Hz), 7.76-7.66 (m, 4H); ^{13}C NMR (300 MHz, DMSO-d_6) δ (ppm): 160.2 (C3), 148.6 (C8), 147.3 (C7), 137.7 (C4), 135.1, 131.4, 131.2, 130.7, 130.0, 129.4, 129.3, 127.8, 127.3, 126.5, 125.5, 124.1, 122.1, 113.56 (C1),112.33 (C1), 80.98 (C2); FT-IR (KBr) υ_{max} (cm^{-1}) 3422, 2925, 2229, 1745, 1640, 1612, 1578, 1525, 1457, 1431, 1041, 757, 722. HRMS (ESI-TOF) m/z: [DCPPI + H]$^{+}$ calcd for C25H14N4 371.1291; Found 371.1292.

(4) Synthesis of adduct DCPPIA: To a solution of **DCPPI** (50 mg, 0.14 mmol) in methanol (5 ml), sodium cyanide (10 mg, 0.2 mmol) was added. The reaction mixture was stirred at room temperature for 30 min. After a complete chemical reaction (monitored on TLC) solvent was removed. The residue was washed with water, filtered and dried in air. The compound was purified by silica gel column chromatography using gradients of hexane/ethyl acetate (90/10 v/v) to afford brown red color solid compound (45 mg; 84% Yield); Mp: ~ 315-320^{o}C, R_f = 0.7 (hexane : EtOAc 7 : 3, v/v); ^{1}H NMR (300 MHz, DMSO-d_6) δ (ppm): 13.68 (s, 1H, NH), 8.896-8.867 (t, 2H, J_1 = 8.7 Hz, J_2 = 7.8 Hz, H4 proton), 8.60-8.545 (t, 2H, J_1 = 7.8 Hz, J_2 = 8.7 Hz, H2 proton), 8.47 (m, 2H, H7 proton), 8.199-8.172 (d, 2H, J = 8.1 Hz, H3 proton), 7.762-7.651 (m, 4H, H5 & H6 proton), 4.07 (s, 1H, Hv'), 3.91 (s, 1H, Hv''); ^{13}C NMR (75 MHz, DMSO-d_6)**:** δ (ppm); 148.49 (C8'), 146.66 (C7'), 137.17 (C4'), 130.5, 129.9, 129.3, 127.8, 127.6, 127.2, 126.1, 125.9, 125.5, 125.3, 124.1, 123.7, 122.4, 121.9, 114.3 (C1'), 114 (C1'), 113.7 (C1"), 29.03 (C3'), 23.7 (C2'); FT-IR (KBr) υ_{max} (cm^{-1}) 3339, 2923, 2853, 2194, 1656, 1614, 1551, 1482, 1456, 1426, 1235, 1111, 755, 723; HRMS (ESI-TOF) m/z: [DCPPIA + H]$^{+}$ calcd for C26H15N5 398.1403; Found 398.1402.

List of Abbreviations

ICT = intramolecular charge transfer

DCPPI = dicyanovinylphenanthroimidazole

DCPPIA = dicyanovinylphenanthroimidazole adduct

CH_2Cl_2 = dichloromethane (DCM)

$CHCl_3$ = chloroform

DMF = *N,N'*-dimethylformamide

EtOH = ethanol

MeOH = methanol

$AcONH_4$ = ammonium acetate

AcOH = acetic acid

TEA = triethylamine

NaCN = sodium cyanide

Conflict of interest

The authors confirm that this article content has no conflict of interest.

Notes: †Authors have made equal contribution

Acknowledgment

Authors are thankful to the Council of Scientific and Industrial Research (CSIR) New Delhi for financial assistance and fellowships (MS, RA, SSR and PS). Authors are also thankful to The Head, Department of Chemistry for generating necessary facilities.

Supporting Information Available: General experimental detail, ^{1}H, ^{13}C NMR, FTIR, ESI-MS, HRMS, absorption, emission, and theoretical data.

References

[1] Martinez-Manez, R.; Sancenon, F. Fluorogenic and chromogenic chemosensors and reagents for anions. *Chem. Rev.,* **2003**, *103*, 4419-4476.

[2] Xu, Z.; Kim, S. K.; Yoon, J. Revisit to imidazolium receptors for the recognition of anions: highlighted research during 2006–2009. *Chem. Soc. Rev*., **2010**, *39*, 1457-1466.

[3] de Silva, A. P.; Gunaratne, H. Q. N.; Gunnlaugsson, T.; Huxley, A. J. M.; McCoy, C. P.; Rademacher, J. D.; Rice, T. E. Signaling recognition events with fluorescent sensors and switches. *Chem. Rev*., **1997**, *97,* 1515-1566.

[4] P. A Gale, Anion and ion-pair receptor chemistry: highlights from 2000 and 2001. *Coord. Chem. Rev*., **2003**, *240,* 191-221.

[5] J. L. Sessler,; S. Camiolo,; P. A. Gale. Pyrrolic and polypyrrolic anion binding agents. *Coord. Chem. Rev.* **2003**, *240*, 17-55.

[6] Lakowicz, J. R.; ‘‘*Principles of Fluorescence Spectroscopy’’*, 3rd edition, Springer, New York **2006**.

[7] Suksai, C.; Tuntulani, T. Chromogenic anion sensors. *Chem. Soc. Rev.,* **2003**, *32*, 192-202.

[8] Kulig, K. W. *Cyanide Toxicity*; U.S. Department of Health and Human Services: Atlanta, GA, **1991**. [9] Young, C.; Tidwell, L.; Anderson, C. *Cyanide: social, industrial, and economic aspects; minerals, metals, and materials society*: Warrendale, **2001**.

[10] Kim, H. J.; Lee, H.; Lee, J. H.; Choi, D. H.; Jung, J. H.; Kim, J. S. Bisindole anchored mesoporous silica nanoparticles for cyanide sensing in aqueous media. *Chem. Commun*., **2011**, *47,* 10918-10920.

[11] Shahid, M.; Misra, A. A simple and sensitive intramolecular charge transfer fluorescent probeto detect CN^- in aqueous media and living cells. *Anal. Methods,* **2013**, *5*, 434-437.

[12] Wang, F.; Wang, L.; Chen, X.; Yoon, J. Recent progress in the development of fluorometric and colorimetric chemosensors for detection of cyanide ions. *Chem. Soc. Rev.,* **2014**, *43*, 4312-4324.

[13] Hudnall, T. W.; Chiu, C.-W.; Gabbai, F. P. Fluoride Ion Recognition by Chelating and Cationic Boranes. *Acc. Chem. Res*., **2009**, *42*, 388-397.

[14] Schwarzenbach, R.; Escher, B. I.; Fenner, K.; Hofstetter, T. B.; Johnson, C. A.; von Gunten, U.; Wehrli, B. The challenge of micropollutants in aquatic systems. *Science.,* **2006**, *313*, 1072-1077.

[15] Xu, Z.; Chen, X.; Kim, H. N.; Yoon, J. Sensors for the optical detection of cyanide ion. *Chem. Soc. Rev*., **2010**, *39*, 127-137.

[16] Chen, X.; Nam, S.-W.; Kim, G.-H.; Song, N.; Jeong, Y.; Shin, I.; Kim, S. K.; Kim, J.; Park, S.; Yoon, J. A near-infrared fluorescent sensor for detection of cyanide in aqueous solution and its application for bioimaging. *Chem. Commun.,* **2010**, *46*, 8953-8955.

[17] Shahid, M.; Razi, S. S.; Srivastava, P.; Ali, R.; Maiti, B.; Misra, A. A useful scaffold based on acenaphthene exhibiting Cu2+ induced excimer fluorescence and sensing cyanide via Cu^{2+} displacement approach. *Tetrahedron* **2012**, *44***,** 9076-9084.

[18] Razi, S. S.; Ali, R.; Srivastava, P.; Shahid M.; Misra A. An efficient multichannel probe to detect anions in different media and its real application in human blood plasma. *RSC Adv*., **2014**, *4,* 22308-22317.

[19] Gunnlaugsson, T.; Kruger, P. E.; Jensen, P.; Tierney, J.; Ali, H. D. P.; Hussey, G. M. Colorimetric "naked eye" sensing of anions in aqueous solution. *J. Org. Chem*., **2005**, *70*, 10875-10878.

[20] Misra, A.; Shahid, M.; Dwivedi, P. An efficient thiourea-based colorimetric chemosensor for naked-eye recognition of fluoride and acetate anions: UV–vis and^{1}HNMR studies. *Talanta.,* **2009**, *80*, 532-538. [21] Dydio, P.; Lichosyt, D.; Jurczak, J. Amide- and urea-functionalized pyrroles and benzopyrroles as synthetic, neutral anion receptors. *Chem. Soc. Rev*., **2011**, *40*, 2971-2985.

[22] Shahid, M.; Srivastava, P.; Misra, A. An efficient naphthalimide based fluorescent dyad (ANPI) for F^{-} and Hg^{2+}mimicking OR, XNOR and INHIBIT logic functions. *New J. Chem*., **2011**, *35*, 1690-1700.

[23] Razi, S. S.; Srivastava, P.; Ali, R.; Gupta, R. C.; Dwivedi, S. K.; Misra A. A coumarin-derived useful scaffold exhibiting Cu^{2+} induced fluorescence quenching and fluoride sensing (On–Off–On) via copper displacement approach. *Sensors and Actuators B*., **2015**, *209*, 162–171.

[24] Aydogan, A.; Coady, D. J.; Lynch, V. M.; Akar, A.; Marquez, M.; Bielawski, C. W.; Sessler, J. L. Poly(methyl methacrylate)s with pendant calixpyrroles: polymeric extractants for halide anion salts. *Chem. Commun*., **2008**, 1455-1457.

[25] Bhaumik, C.; Maity, D.; Das, S.; Baitalik, S. Synthesis, structural characterization, solvatochromism, and ion-binding studies of a ditopic receptor based on 2-(4-[2,2′: 6′,2″] terpyridin-4′-yl-phenyl)-1*H*-phenanthro[9,10-*d*] imidazole (tpy-HImzphen) unit. *RSC Adv*., **2012**, *2*, 2581-2594.

[26] Kumari, N.; Jha, S.; Bhattacharya, S. Colorimetric probes based on anthraimidazolediones for selective sensing of fluoride and cyanide ion via intramolecular charge transfer. *J. Org. Chem.,* **2011**, *76*, 8215-8222.

[27] Gou, Z.; Song, N. R.; Moon, J. H.; Kim, M.; Jun, E. J.; Choi, J.; Lee, J. Y.; Bielawski, C. W.; Sessler, J. L.; Yoon, J. A Benzobisimidazolium-based fluorescent and colorimetric chemosensor for CO_2. *J. Am. Chem. Soc*., **2012**, *134*, 17846-17849.

[28] Hudnall, T. W.; Gabbai, F. P. Ammonium boranes for the selective complexation of cyanide or fluoride ions in water. *J. Am. Chem. Soc*., **2007**, *129*, 11978-11986.

[29] Dong, M.; Peng, Y.; Dong, Y.-M.; Tang, N.; Wang, Y.-W. A selective, colorimetric, and fluorescent chemodosimeter for relay recognition of fluoride and cyanide anions based on 1,1′-binaphthyl scaffold. *Org. Lett*., **2012**, *14*, 130-133.

[30] Nishimura, T.; Xu, S.-Y.; Jiang, Y.-B.; Fossey, J. S.; Sakurai, K.; Bull, S. D.; James, T. D. A simple visual sensor with the potential for determining the concentration of fluoride in water at environmentally significant levels. *Chem. Commun*., **2013**, *49*, 478-480.

[31]Lee, M. H.; Agou, T.; Kobayashi, J.; Kawashima, T.; Gabbai, F. P. Fluoride ion complexation by a cationic borane in aqueous solution. *Chem. Commun*., **2007**, 1133-1135.

[32] Lu, H.; Wang, Q.; Li, Z.; Lai, G.; Jiang, J.; Shen, Z. A specific chemodosimeter for fluoride ion based on a pyrene derivative with trimethylsilylethynyl groups. *Org. Biomol. Chem*., **2011**, *9*, 4558-4562.

[33] Maldonado, C. R.; Touceda-Varela, A.; Jonesa, A. C.; Mareque-Rivas, J. C. A turn-on fluorescence sensor for cyanide from mechanochemical reactions between quantum dots and copper complexes. *Chem. Commun*., **2011**, *47*, 11700-11702.

[34] Guliyev, R.; Ozturk, S.; Sahin, E.; Akkaya, E. U. Expanded bodipy dyes: anion sensing using a bodipy analog with an additional difluoroboron bridge. *Org. Lett.,* **2012,** *14,* 1528-1531.

[35] Mo, H.-J.; Shen, Y.; Ye, B.-H. Selective recognition of cyanide anion via formation of multipoint NH and phenyl CH hydrogen bonding with acyclic ruthenium bipyridine imidazole receptors in water. *Inorg. Chem*., **2012**, *51*, 7174-7184.

[36] Razi, S. S.; Ali, R.; Srivastava, P.; Misra, A. A selective quinoline-derived fluorescent chemodosimeter to detect cyanide in aqueous medium. *Tetrahedron Letters*, **2014,** *55*, 1052–1056.

[37] Lee, K.-S.; Kim, H.-J.; Kim, G.-H.; Shin, I.; Hong, J.-I. Fluorescent chemodosimeter for selective detection of cyanide in water. *Org. Lett.,* **2008**, *10*, 49-51.

[38] Cho, D.-G.; Kim, J. H.; Sessler, J. L. The benzil−cyanide reaction and its application to the development of a selective cyanide anion indicator. *J. Am. Chem. Soc.*, **2008,** *130***,** 12163-12164.

[39] Zou, Q.; Li, X.; Zhang, J.; Zhou, J.; Sun, B.; Tian, H. Unsymmetrical diarylethenes as molecular keypad locks with tunable photochromism and fluorescence via Cu2+ and CN coordinationsw. *Chem. Commun*., **2012**, *48*, 2095-2097.

[40] Chen, X.; Nam, S-W.; Kim, G-H.; Song, N.; Jeong, Y.; Shin, I.; Kim, S. K.; Kim, J.; Park, S.; Yoon, J. A near-infrared fluorescent sensor for detection of cyanide in aqueous solution and its application for bioimaging. *Chem. Commun*., **2010**, *46***,** 8953-8955.

[41] Qu, Y.; Hua, J.; Tian, H.; Colorimetric and ratiometric red fluorescent chemosensor for fluoride Ion based on diketopyrrolopyrrole. *Org. Lett*., **2010**, *12*, 3320-3323.

[42] Lee, M. H.; Kim, J. S.; Sessler, J. L. Small molecule-based ratiometric fluorescence probes focations, anions, and biomolecules. Advanced article. *Chem. Soc. Rev*., **2015.**

[43] Liu, X. Y.; Bai, D. R.; Wang, S. Charge-transfer emission in nonplanar three-coordinate organoboron compounds for fluorescent sensing of fluoride. *Angew. Chem., Int. Ed*., **2006**, *45*, 5475-5478.

[44] Swamy, K. M. K.; Lee, Y. J.; Lee, H. N.; Chun, J.; Kim, Y.; Kim, S.-J.; Yoon, J. A new fluorescein derivative bearing a boronic acid group as a fluorescent chemosensor for fluoride ion. *J. Org. Chem*., **2006,** *71*, 8626-8628.

[45] Day, A. R.; Steck, E. A. Reactions of phenanthraquinone and retenequinone with aldehydes and ammonium acetate in acetic acid solution. *J. Am. Chem. Soc*., **1943,** *65*, 452-456.

[46] Krebs, F. C.; Jørgensen, M. A new versatile receptor platform. *J. Org. Chem.*, **2001**, *66*, 6169-6173. [47] Bu, L.; Sawada, T.; Kuwahara, Y.; Shosenji, H.; Yoshida, K. Crystallographic structure and solid-state fluorescence enhancement behavior of a 2-(9-anthryl)phenanthroimidazole-type clathrate host upon inclusion of amine molecules. *Dyes Pigm*., **2003**, *59*, 43-52.

[48] Krebs, F. C.; Lindvold, L. R., Jorgensen, M. J. Superradiant properties of 4,4′-bis(1*H*-phenanthro[9,10-*d*]imidazol-2-yl)biphenyl and how a laser dye with exceptional stability can be obtained in only one synthetic step. *Tetrahedron Lett.,* **2001**, *42*, 6753-6757.

[49] Noormofidi, N.; Slugovc, C. Acid/base-sensitive ring-opening metathesis polymers based on phenanthroimidazole dyes. *Macromol. Chem. Phys*., **2007,** *208*, 1093–1100.

[50] Zhanga, Y.; Ng, T-W.; Lua, F.; Tonga, Q.-X.; Lai, S.-L.; Chanc, M.-Y.; Kwong, H.-L.; Lee, C-S. A pyrene-phenanthroimidazole derivative for non-doped blue organic light-emitting devices. *Dyes Pigm.*, **2013,** *98*, 190-194.

[51] Benelhadj, K.; Massue, J.; Retailleau, P.; Ulrich, G.; Ziessel, R. 2‑(2'-Hydroxyphenyl) benzimidazole and 9,10-phenanthroimidazole chelates and borate complexes: solution- and solid-state emitters *Org. Lett.*, **2013,** *15*, 2918-2921.

[52] Zhanga, X.; Linb, J.; Ouyanga, X.; Liua, Y.; Liub, X.; Gea, Z. J. Novel host materials based on phenanthroimidazole derivatives for highly efficient green phosphorescent OLEDs. *Photochem. Photobiol.*, **2013**, *268*, 37-43.

[53] Zheng, K.; Lin, W.; Tan, Li. A phenanthroimidazole-based fluorescent chemosensor for imaging hydrogen sulfide in living cells. *Org. Biomol. Chem.*, **2012**, *10*, 9683-9688.

[54] Song, K. C.; Kim, H.; Lee, K. M.; Lee, Y. S.; Do, Y.; Lee, M. H. Ratiometric fluorescence sensing of fluoride ions by triarylborane-phenanthroimidazole conjugates. *Sens Actuators B,* **2013**, *176***,** 850-857.

[55] Zhuang, S.; Shangguan, R.; Jin, J.; Tu, G.; Wang, L.; Chen, J.; Ma, D.; Zhu, X. Efficient nondoped blue organic light-emitting diodes based on phenanthroimidazole-substituted anthracene derivatives. *Organic Electronics*., **2012,** *13*, 3050-3059.

[56] Song, K. C.; Choi, M. G.; Ryu, D. H.; Kim, K. N.; Chang, S-K. Ratiometric chemosensing of Mg^{2+} ions by a calix[4]arene diamide derivative. *Tetrahedron. Lett.* **2007**, *48*, 5397-5400.

[57] Sluys, W. G. V. D. *J.* The solubility rules: Why are all acetates soluble? *Chem. Educ*., **2001**, *78*, 111. [58] Marcus, Y. Thermodynamics of solvation of ions. *J. Chem. Soc. Faraday Trans*., **1991**, *87*, 2995-2999.

[59] Misra, A.; Shahid, M. Chromo and fluorogenic properties of some azo-phenol derivatives and recognition of Hg^{2+} ion in aqueous medium by enhanced fluorescence. *J. Phys. Chem. C*., **2010**, *114*, 16726-16739.

[60] Misra, A.; Srivastava, P.; Shahid, M. Fluorescent probe mimicking multiple logic gates and a molecular keypad lock upon interaction with Hg^{2+} and bovine serum albumin. *Analyst*., **2012**, *137*, 3470-3478.

[61] Srivastava, P.; Shahid, M.; Misra, A. Protein assisted fluorescence enhancement of a dansyl containing fluorescent reagent: Detection of Hg^{+} ion in aqueous medium. *Org. Biomol. Chem*., **2011,** *9*, 5051-5055.

[62] Misra, A.; Shahid, M.; Srivastava, P. Optoelectronic behavior of bischromophoric dyads exhibiting Zn^{2+}/F^{-} ions induced "*turn-On/Off*" fluorescence. *Sens. Actuators B*, **2012,** *169*, 327-340.

[63] Srivastava, P.; Ali, R.; Razi, S. S.; Shahid, M.; Misra, A. Thiourea based molecular dyad (ANTU): Fluorogenic Hg^{2+} selective chemodosimeter exhibiting blue–green fluorescence in aqueous-ethanol environment. *Sens. Actuators B*, **2013,** *181*, 584-595.

[64] Pandey, R.; Gupta, R. K.; Shahid, M.; Maiti, B.; Misra, A.; Pandey, D. S. Synthesis and Characterization of Electroactive Ferrocene Derivatives: Ferrocenylimidazoquinazoline as a Multichannel Chemosensor Selectively for Hg^{2+} and Pb^{2+} Ions in an Aqueous Environmen. *Inorg. Chem.***, 2012,** *51*, 298-311.

[65] Razi, S. S.; Ali, R.; Srivastava, P.; Misra, A. Simple Michael acceptor type coumarin derived turn-on fluorescence probes to detect cyanide in pure water. *Tetrahedron Lett.,* **2014,** *55*, 2936-2941.

[66] Srivastava, P.; Ali, R.; Razi, S. S.; Shahid, M.; Patnaik, S.; Misra, A. A simple blue fluorescent probe to detect Hg^{2+} in semiaqueous environment by intramolecular charge transfer mechanism**.** *Tetrahedron Lett*., **2013,** *54*, 3688–3693.

[67] Furniss, B. S.; Hannaford, A. J.; Smith, P.W.G.; Tatchell, A. R. Vogel's textbook of practical organic chemistry, Fifth edition, pp 1023-1024.

[68] Hijji, Y. M.; Barare, B.; Kennedy, A. P.; Butcher, R. Synthesis and photophysical characterization of a Schiff base as anion sensor. *Sens Actuators B*, **2009,** *136*, 297-302.

[69] Boiocchi, M.; Boca, L. D.; Gomez, D. E.; Fabbrizzi, L.; Licchelli, M.; Monzani, E. Nature of urea-fluoride interaction: incipient and definitive proton transfer. *J. Am. Chem. Soc.*, **2004,** *126*,16507-16514.

[70] Benesi, H. A.; Hildebrand, J. H. A spectrophotometric investigation of the interaction of iodine with aromatic hydrocarbons. *J. Am. Chem. Soc*., **1949**, *71,* 2703-2707.

[71] Connors, K.A. Binding constant, 1st ed., Wiley, New York, **1987**.

[72] Yang, Y.; Zhao, Q.; Feng, W.; Li, F. Luminescent chemodosimeters for bioimaging. *Chem. Rev*., **2013**, *113*, 192−270.

[73] Frisch, M. J.; Truncks, G. W.; Schlegel, H. B. *GAUSSIAN 03, Revision E.01,* Gaussian Inc., Wallingford, CT, **2007.**